Hindawi
Advances in Polymer Technology
Volume 2019, Article ID 8156718, 10 pages
https://doi.org/10.1155/2019/8156718

Research Article

The Effect of Interaction between Nanofillers and Epoxy on Mechanical and Thermal Properties of Nanocomposites: Theoretical Prediction and Experimental Analysis

S. Khostavan,[1] **M. Fazli**,[1] **M. Ghorbanzadeh Ahangari**,[2] **and Y. Rostamiyan**[3]

[1]*Department of chemistry, Faculty of Science, Semnan University, Semnan, Iran*
[2]*Department of Mechanical Engineering, Faculty of Engineering and Technology, University of Mazandaran, Babolsar, Iran*
[3]*Department of Mechanical Engineering, Sari Branch, Islamic Azad University, Sari, Iran*

Correspondence should be addressed to M. Fazli; mfazli@semnan.ac.ir

Received 30 July 2018; Accepted 24 March 2019; Published 2 May 2019

Academic Editor: Anil K. Bhowmick

Interfacial interaction between host matrix and nanofillers is a determinative parameter on the mechanical and thermal properties of nanocomposites. In this paper, we first investigated interaction between carbon nanotube (CNT) and montmorillonite clay (MMT) absorbing on epoxy surface in a theoretical study based on the density functional theory (DFT) calculations. Results showed the interaction energy of -1.93 and -0.11 eV for MMT/epoxy and CNT/epoxy, respectively. Therefore, the interaction between epoxy polymer and MMT is of the chemisorptions type, while epoxy physically interacts with CNT. In addition, thermal and mechanical analyses were conducted on nanocomposites. In DSC analysis the glass transition temperature which was 70°C in neat epoxy composite showed an improvement to about 90°C in MMT nanocomposites while it was about 70°C for CNT nanocomposites. Finally, mechanical properties were investigated and MMT nanocomposite showed a change in compressive strength which increased from 52.60 Mpa to 72.07 and 92.98 Mpa in CNT and MMT nanocomposites, respectively. Also tensile strength improved to the value of 1250.69 Mpa MMT nanocomposites while it was about 890 Mpa in both CNT nanocomposite and neat epoxy composite which corresponds to the calculation result prediction.

1. Introduction

Epoxy matrix composites are one of the most common thermosetting polymers that are widely used because of properties including solvent resistance, thermal stability, and high tensile strength and still new research continues to improve these properties [1–6]. These characteristics made epoxy composites to be used in industrial applications such as adhesives, coatings, electronics, encapsulation, and laminates. To improve the aforesaid properties nanofillers are introduced to epoxy matrix which is examined by mechanical and thermal analysis of neat polymer and nanocomposites to monitor change of nanofiller curing [7–10]. A promising method to study the efficiency of nanofillers is calculating interfacial interaction between the nanofiller and the polymer matrix that can facilitate and reduce costs of unnecessary tests. The factors that play a major role in the properties of nanocomposites are nanoparticle-matrix interaction and particle-particle interaction. The quality of interface and the strength of the adhesion at the interface provide load transfer between the host matrix and the nanofillers. Also in case of increased interfacial binding, mechanical properties of the nanocomposites would be improved. So it would be pleasant to estimate the interfacial interaction energy. As it is difficult to approximate interfacial interaction in experiments calculation methods can be a good option. There are different calculating methods such as molecular mechanics (MM), molecular dynamics (MD), and ab initio quantum mechanical methods [11–15]. Among them ab initio quantum mechanical calculations provide more accurate results than other classical methods. Hartree-Fock (H–F) and density functional theory (DFT) calculations are two ab initio quantum mechanics methods and in the case of large number of atoms DFT method is very efficient [16–21].

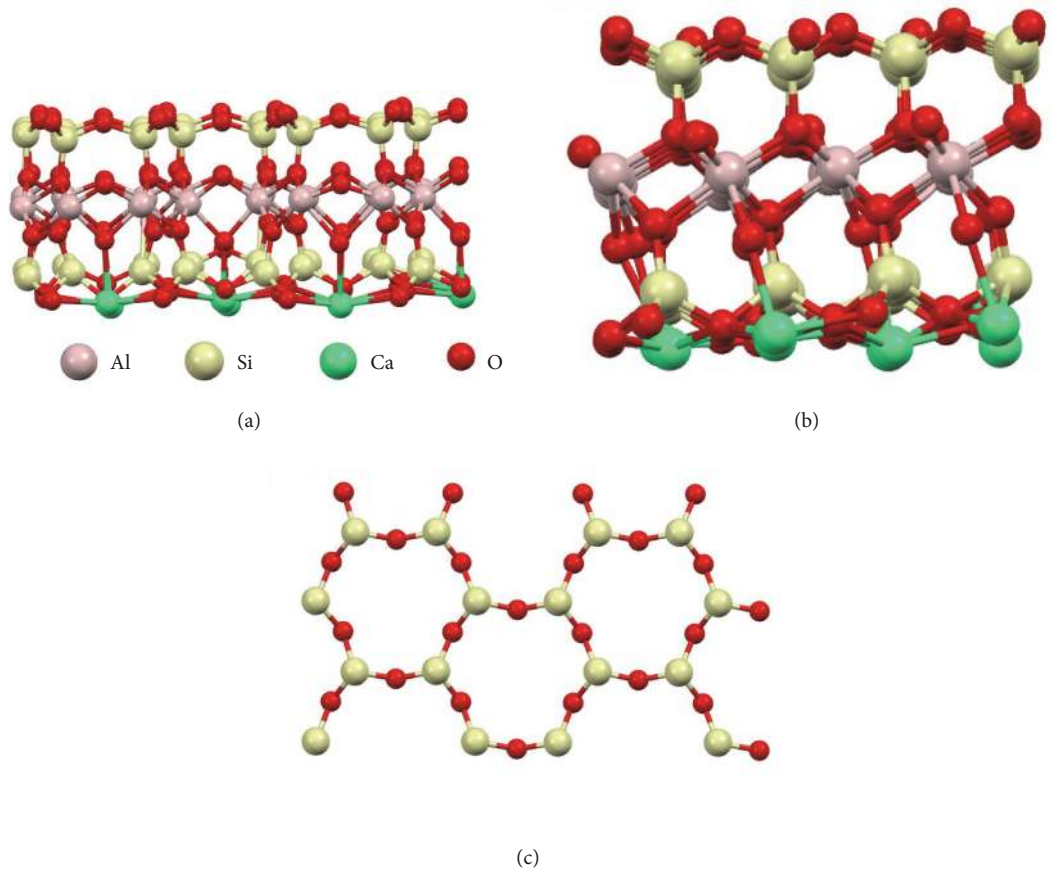

Figure 1: Super cell of montmorillonite. (a) front view, (b) side view, and (c) top view.

In many cases, the results from the DFT calculations for solid-state systems agree quite satisfactorily with experimental data. Therefore, the interaction between different types of nonmaterial as fillers and the epoxy polymers can be studied using this method. In an investigation accomplished by Ghorbanzadeh et al. [22], the interaction of epoxy monomer with different types of SWCNTs was studied using DFT calculations, in which the calculated results of interaction energy values showed weak binding between the epoxy and different types of SWCNTs that was in the range of -0.05 to -0.22 eV and typical for the physisorption. The adsorption of the epoxy monomer on the surface of the functionalized nanotube indicated that –OH and $–NH_2$ functional groups increase the physisorption capability of the nanotube to approximately -0.41 and -0.38 eV.

The aim of the present work was to predict and compare the interaction between epoxy matrix and SWCNTs and clay as fillers using calculation methods and then proof the results by experimental methods. DFT calculations were used to estimate interaction between epoxy matrix and nanofillers, and the accuracy of the results was tested by mechanical and thermal properties of two different nanocomposites.

2. Methodology

2.1. Structural Models and Force Field Parameters. Both systems were optimized by the self-consistent charge density functional tight-binding (SCC-DFTB) calculations implemented in the DFTB+ program package [23, 24]. The geometrical optimizations were performed using the conjugate gradient algorithm and the total energy calculations of the systems were accomplished inside the framework of DFT, as implemented in the Spanish Initiative for Electronic Simulations with Thousands of Atoms (SIESTA) code [25–28]. The exchange and correlation potential were obtained utilizing a generalized gradient approximation (GGA) with the Perdew–Burke–Ernzerhof (PBE) functional theory [29]. All of the calculations were solved using a double-z plus polarization (DZP) basis set with an energy shift of 50 meV. Along the CNT tubes, k-points were used for the axes with a $1 \times 1 \times 5$ Monkhorst Packgrid for the Brillouin zone integration.

The montmorillonite model is based on a $5.180 \times 8.980 \times 15.000$ Å^3 unit cell structure obtained by single crystal X-ray refinement [30] and the initial unit cell was replicated ($2 \times 2 \times 1$) along a, b, and c crystallographic directions, respectively. This resulted in a super cell MMT layer of a total of 4 unit cells (Figures 1(a), 1(b), and 1(c)) and the k-points were used for the axes with a $5 \times 5 \times 1$ Monkhorst–Pack grid.

The mesh cut-off was chosen to be 120 Ry for all calculations. Adding ghost atoms to the calculation of the isolated absorbent, the basis set superposition error (BSSE) was eliminated [31]. By employing basic functions the ghost atoms do not affect the calculation. Hence the same degrees of freedom are available to the wave functions in all of

the calculations. This procedure is named the counterpoise method. The interaction energy for the absorption of the epoxy onto the nanofillers surface was achieved through the following expression:

$$E_i = E_{(nanofiller\text{-}epoxy)} - E_{(nanofillerghost\text{-}epoxy)} - E_{(nanofiller\text{-}epoxyghost)} \quad (1)$$

where E_i is the total energy of the nanofiller interacting with the epoxy polymer. The $E_{\text{'ghost' nanofiller/epoxy}}$ correspond to the counterpoise method.

3. Experimental

3.1. Materials. As a matrix for preparing a polymeric nanocomposite, D. E. R. 332 epoxy resin from Sigma Aldrich with an epoxy equivalent weight of 175 equiv. g^{-1} was used. Triethylenetetramine, which is a liquid aliphatic amine with a molecular weight of 146.24 $g.mol^{-1}$ and density of 0.977 $g.mol^{-1}$ at 20°C, was used as a hardener and was purchased from Merck. SWCNT was purchased from Sigma Aldrich and used without further purification. The average diameter of the used SWCNT was 0.78 nm and its purity was more than 95%. Natural MMT was also purchased from Sigma Aldrich.

3.2. Sample Preparation. 40 g of epoxy was heated at 50°C and then optimum weight of nanofiller dispersed into the solution by mechanical stirrer in 10 min. In the next step, a stoichiometric ratio of the diamine was added to the mixture and stirred mechanically for additional 10 min and finally ultrasonicated for approximately 15 min. The samples were prepared, molded, and placed in vacuum for 15 minutes in ambient temperature, afterward cured in two cases: for about 30 min in 60°C and then 1 hour in 100°C. Neat epoxy specimens were prepared as the same method.

3.3. DSC Analysis. The optimum weight of nanofiller was obtained by determining the reaction enthalpy of the exothermic peak on dynamically cured samples involving various nanofiller concentrations (0%, 1%, 3%, 5%, 10%, and 15%). The amounts of MWCNT and MMT were selected 5% and 10%, respectively, based on the maximum value of ΔH in DSC measurements. A NETZSCH DSC 200 F3 unit was employed for calorimetric analysis. Dynamic DSC experiments were conducted in nitrogen atmosphere at temperature range of 25–300°C at constant heating rate of 20°C.min^{-1} and then reheated from 25 to 250 by the heating rate of 10°C.min^{-1} to investigate glass-transition temperature for each sample. DSC samples were prepared for one gram of epoxy.

3.4. Tensile Test. Samples were tested by a Santam testing unit. The gauge length was 50 mm. The tensile tests were conducted at 0.5 and 2 mm.min^{-1} of cross head speed, and the elongation of the gauge length was measured by a noncontact extensometer. At least five specimens from nanocomposites were used for the experiments.

Table 1: Interaction energy and the equilibrium distances between the closest atom of the epoxy and the layer of montmorillonite.

System	$D_{epoxy\text{-}MMT}$(Å)	E_i (eV)
Site 1	2.03	-0.7
Site 2	2.1	-1.93

3.5. Compressive Properties Test. Samples were tested by a Santam testing unit. The gauge length was 12 mm. The compressions were applied at 0.25 mm.min^{-1} of cross head speed and the elongation of the gauge length was measured by a noncontact extensometer. Compression tests were conducted on the 12.5 × 12.5 × 25.4 mm^3 cube specimens (according to ASTM standard D695-96) and at least five specimens were tested for each system.

3.6. Scanning Electron Microscopy (SEM). SEM micrographs on the fracture surface of the epoxy nanocomposite were obtained with a Tescan Scanning Electron Microscope (SEM) operated at 10 kV. In order to observe the images clearly, a thin film of gold was sputtered at 10 mA for 45 s on the surface of the probe using a Hummer 600 sputtering system.

4. Results and Discussion

4.1. Interaction Energy between the Epoxy Monomer and SWCNTs. DFT calculations were performed to determine the influence of nanotube on epoxy desorption in bisphenol A epoxy monomer and (10, 0) SWCNT systems. The diameter and length of SWCNT were 7.774 Å and 20.44 Å, respectively. The interaction energy calculated for the situation that epoxy monomer approached the sidewall of the carbon nanotube (Figures 2(a) and 2(b)) and the result for the epoxy monomer absorbed on the surface of the nanotube was -0.11 eV for the stable configuration of (10,0) nanotube as was also published in a work by Ghorbanzadeh et al. [22]. Figure 2 demonstrates different situation epoxy monomer approaching to SWCNT.

4.2. Interaction Energy between the Epoxy Monomer and Montmorillonite. The interaction energy of epoxy approaching to the TOT plane of montmorillonite was calculated (Figure 3) and Table 1 shows the optimized results for the epoxy monomer absorbed on the epoxy/MMT system along with the interaction energies and the equilibrium distances between the closest atom of the epoxy and the layer of montmorillonite in different situation of epoxy monomer approaching the surface of MMT. As it can be concluded from the data in Table 1 the best interaction energy is -1.93 which corresponds to a situation that epoxy has more interfacial surface with MMT. The interaction energy of the system is obviously higher than the interaction energy between epoxy and carbon nanotube and its value indicates the chemical absorption of epoxy on the clay which can be due to more adhesion.

4.3. Electronic Properties

4.3.1. Density of States (DOS) Calculations. The behavior of electrons in solids depends on the distribution of energy

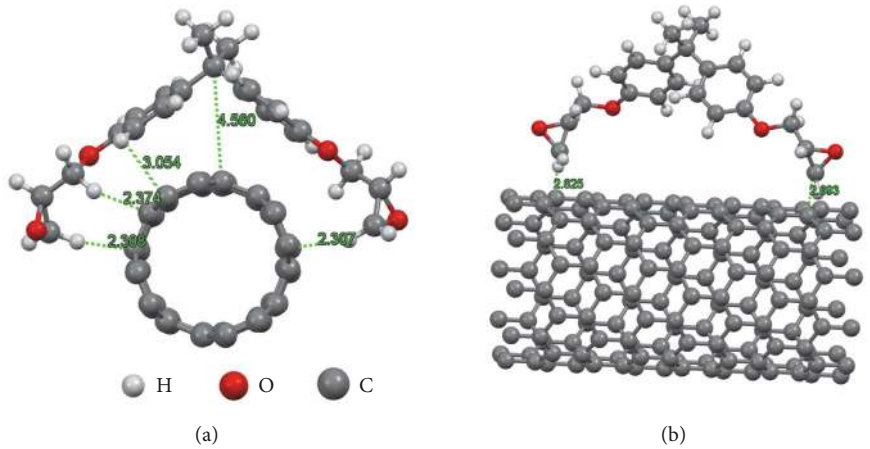

Figure 2: Epoxy monomer approached the sidewall of the carbon nanotube.

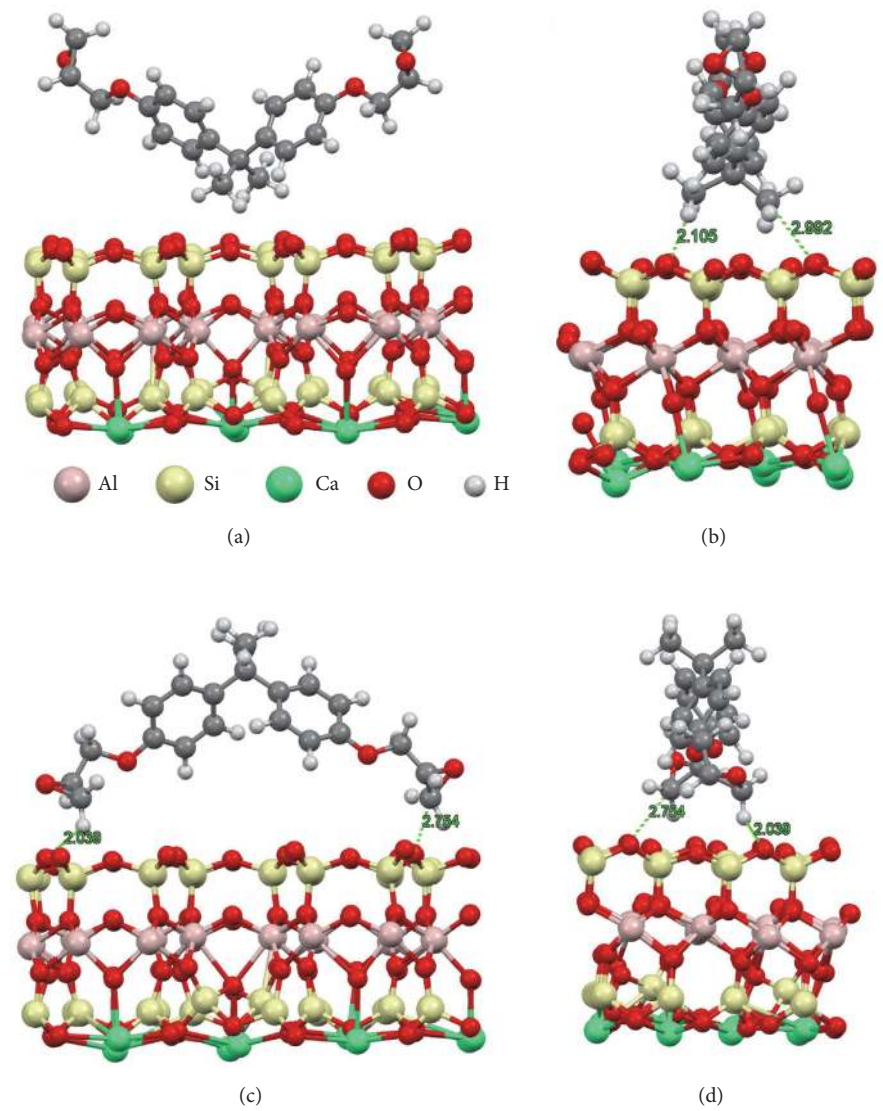

Figure 3: Different situations epoxy monomer approached the surface of MMT and the equilibrium distances between the closest atom of the epoxy and the layer of montmorillonite.

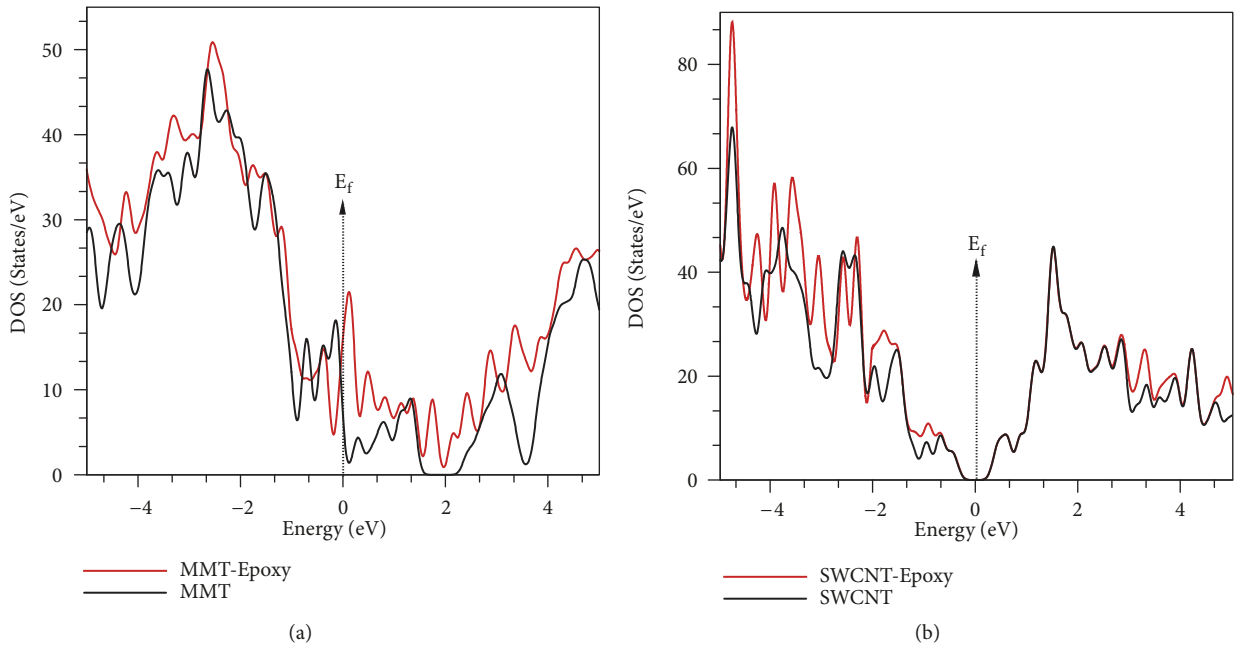

Figure 4: DOS diagrams of (a) montmorillonite nanoparticles and epoxy-montmorillonite nanocomposite and (b) SWCNT and Epoxy-SWCNT.

among the electrons. This distribution determines the probability that a given energy state will be occupied, but must be multiplied by the density of states function to weight the probability by the number of states available at a given energy [32]. Figure 4 presents the total electronic density of states (DOS) between −5 and 5 eV, where the Fermi level (E_f) is set at 0 eV for systems. DOS near the Fermi level is not affected by the adsorption of epoxy monomer on CNT surface, and the DOS of the combined system is nearly a superposition of the DOS of the individual parts. Therefore, the interaction between the epoxy monomer and the nanotube is weak. In contrast, DOS in Fermi level is affected by adsorption of MMT on epoxy and shows increased intensity. Furthermore, DOS in HOMO and LUMO shifted to Fermi level. Result indicates that epoxy adsorption induces a resonant peak near the Fermi level, which can reveal electron transfer from MMT to epoxy in adsorbing process [33].

4.3.2. Mullikan Population Analysis. Mullikan population analysis is also accomplished and the results show 0.37 e transfer from MMT to epoxy monomer. This is in fact more than CNT-epoxy system which was 0.2 e. Mullikan population results also show stronger interaction between MMT and epoxy.

4.4. Experimental

4.4.1. DSC Studies. Differential Scanning Calorimetry can investigate various characteristics of thermosetting composites such as temperature and calories in curing reaction. Also DSC technique is one of the most common methods to study α-transition of polymer composites and nanocomposites [34]. In this study DSC analysis was employed to find the optimum loading for SWCNT and MMT in epoxy. Figures 5 and 6 show the dynamic DSC curves of 0, 1, 3, 5, 10, and 15% of weight of SWCNT and MMT epoxy nanocomposites. The exothermic peak, cure, and glass-transition temperatures of all the studied systems are summarized in Table 2. From data obtained in DSC analysis of different loadings of SWCNT and MMT, optimum value of SWCNT and MMT was chosen to be 5 and 10% of weight.

Obviously a better correction of the glass-transition temperature is observed in the MMT nanocomposite which reached from about 70°C in neat epoxy to about 90°C in MMT nanocomposite (detailed results are presented in Table 2). The change in the glass transition temperature was also interpreted as a result of effective interaction between polymeric chain and nanofillers. In case of attractive forces between the filler and the interfacial polymer, the mobility of the polymer chains is reduced and the glass transition temperature would increase [35, 36]. Better thermal behavior of MMT in comparison with CNT nanocomposites, results from better curing of MMT in epoxy matrix which matches with results of DFT calculations.

4.4.2. Tensile Strain and Compressive Properties. Tensile tests of neat epoxy, CNT, and MMT/epoxy nanocomposites specimens were conducted in two different speeds of 0.5 and 2 mm.min^{-1} in order to measure their tensile properties and the results are summarized in Table 3.

Figures 7 and 8 exhibit the tensile parameter values of neat epoxy and nanocomposites made with optimum value of SWCNT and MMT. It can be considered that tensile strengths in epoxy matrix polymers are sensitive to the speed of the test and tensile modulus values tend to increase by reducing the speed. For neat epoxy and CNT nanocomposites in both

Table 2: Data from dynamic DSC measurements on neat epoxy and CNT/MMT epoxy composites having different loadings of nanofillers.

Mass fraction	0%	CNT					MMT				
		1%	3%	5%	10%	15%	1%	3%	5%	10%	15%
ΔH_T/J.g^{-1}	-470.4	-410.7	-420.8	-446.6	-375.3	-358.1	-417.1	-432.0	-443.8	-458.2	-437.5
Tg/°C	76.17	72.3	73.28	73.47	72.02	69.40	77.16	79.51	85.34	89.20	79.60
Peak onset/°C	55	55	55	55	55	55	60	60	60	60	60
Peak cure max/°C	100	95.9	92.3	88.8	90.0	90.0	96.2	94.1	93.5	93,5	94

Table 3: Tensile strength properties of block specimens: neat, MMT, and CNT epoxy composites.

Content	Neat Epoxy		CNT- Epoxy		MMT-Epoxy	
Rate, mm.min^{-1}	0.5	2	0.5	2	0.5	2
Bending strength, MPa	886.28	670.39	894.05	697.60	1250.69	977.42
Bending modulus, GPa	1.71	1.540	2.040	3.095	1.518	1.485
Elongation ε, %	2.55	2.13	2.14	2.23	7.58	3.79
Stress, MPa	36.63	27.71	36.95	28.83	58.37	40.40

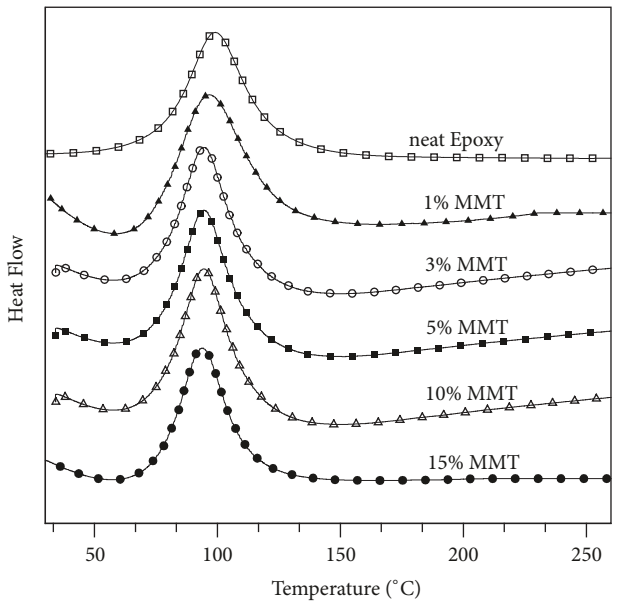

Figure 5: DSC curves of 0, 1, 3, 5, 10, and 15% Weight of MMT-epoxy nanocomposites.

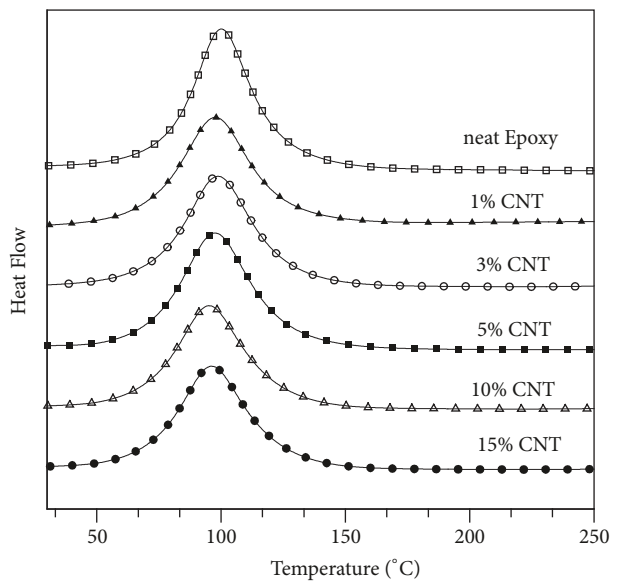

Figure 6: DSC curves of 0, 1, 3, 5, 10, and 15% Weight of SWCNT-epoxy nanocomposites.

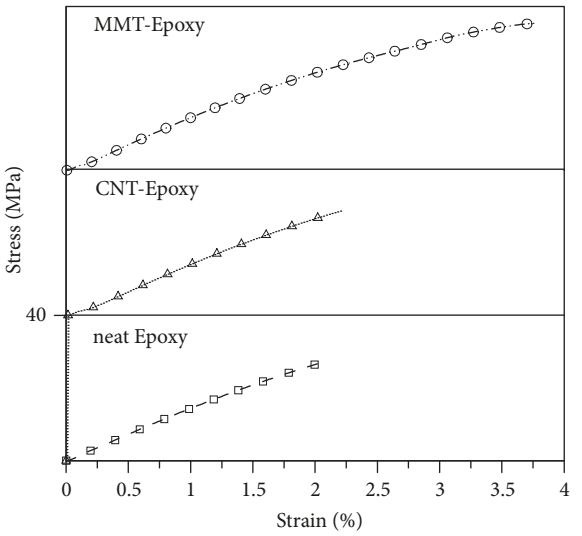

Figure 7: Stress strain graphs of neat epoxy and MMT/ SWCNT-epoxy in optimum fraction, conducted at 2 mm.min^{-1} of cross head speed.

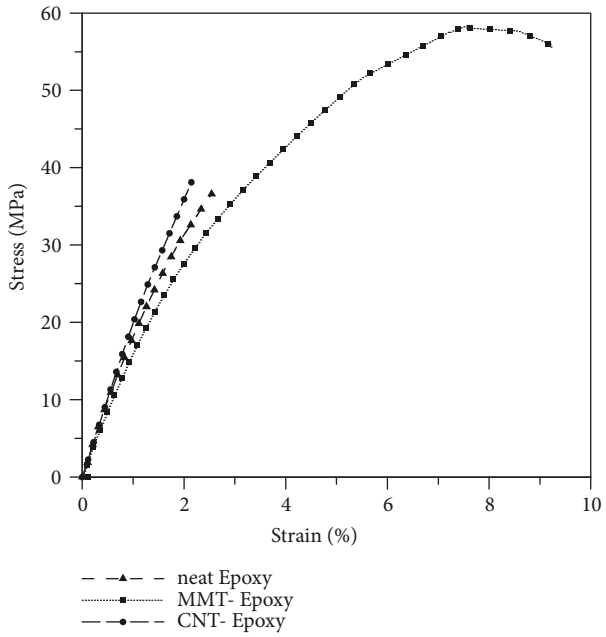

Figure 8: Stress strain graphs of neat epoxy and MMT/SWCNT-epoxy in optimum fraction, conducted at 0.5 mm.min^{-1} of cross head speed.

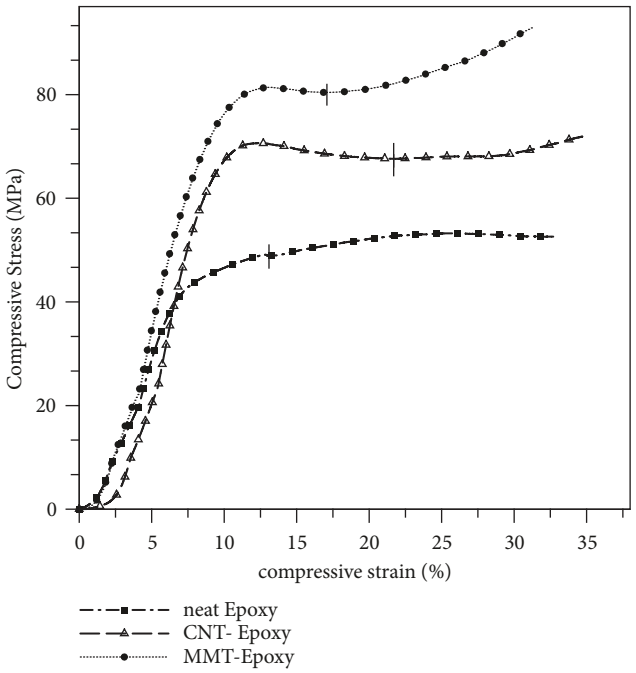

Figure 9: Compressive stress-strain curves of neat epoxy and MMT/SWCNT-epoxy in optimum fraction, conducted at 0.25 mm.min^{-1} of cross head speed.

speeds the tensile stress is maximum at the breaking point, and ultimate tensile strength and strain at break is almost unaffected by adding CNT to epoxy matrix, while ultimate tensile strength and strain at break dramatically increased in MMT nanocomposite and the strain-stress behavior in speed of 0.5 is completely different from CNT and neat composites.

The results show both systems to be Fragile, so the compressive properties, which are good way to study fragile systems, were also used to measure the performance of nanocomposites.

Typical true stress-strain curves of cubic specimens loaded in static uniaxial compression were illustrated in Figure 9. This figure shows the effect of optimum concentration of MMT and SWCNT on the compressive stress-strain behavior of epoxy. It was founded that both MMT and CNT enhanced the compressive strength of the epoxy. The results of compression content are summarized in Table 4.

Nanoparticle-matrix interaction plays a major role in the properties of nanocomposites. The attraction forces between particles, due to the Van der Waals and electrostatic forces, affect the particle-particle interaction and deteriorate the composite's performances and improved mechanical properties can be achieved through improved interface between the particle and matrix [37].

4.4.3. Morphology Study. Scanning Electron Microscopy is used to reveal micro-structural information of fractured surfaces of composites. Figures 10 and 11 show SEM micrographs of fractured surface of CNT-epoxy and MMT-epoxy, respectively. The SWCNT/epoxy has shown uniform dispersion of SWCNT in epoxy matrix. SEM micrographs have shown

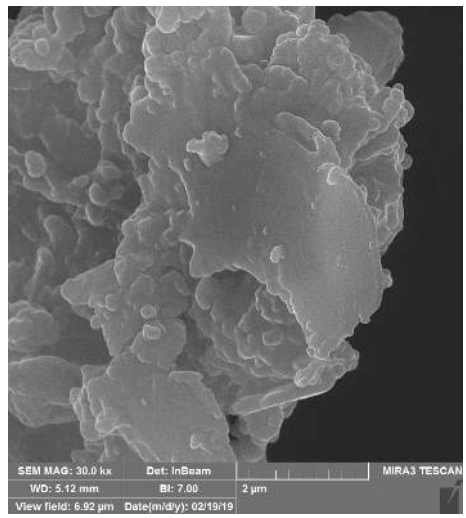

Figure 10: SEM fractograph of 5 wt. % SWCNT nanocomposite.

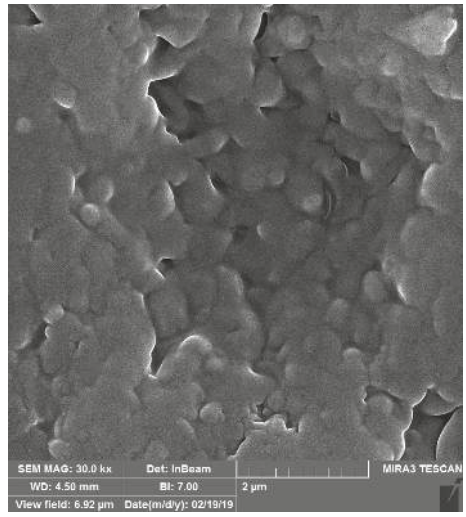

Figure 11: SEM fractograph of 10 wt. % MMT nanocomposite.

dispersed montmorillonite in the matrix and the dispersion was found to be homogeneous. Some places also show the aggregated particles of the dispersal of individual silicate layers. This method investigated a small volume of bulk material in the overall morphology which the presence of such clay aggregates in the microstructure of nanocomposites is also reported by Kornmann et al. [38] and Yasmin et al. [39].

5. Conclusion

In this study, the interaction energy of the bisphenol A epoxy monomer with two different nanofillers (SWCNT and montmorillonite) was assessed using DFT calculations. The calculated interaction energy for these two epoxy systems in the best situation was -0.11 eV for epoxy-SWCNT and -1.9 eV for montmorillonite epoxy nanocomposite. Calculated results showed that among two nanofillers the epoxy

Table 4: The compressive properties of neat, MMT, and CNT epoxy composites.

Compressive property	Neat Epoxy	CNT- Epoxy	MMT-Epoxy
Elastic modulus, E (MPa)	735.19	342.41	225.60
Compressive strength, σu (MPa)	52.60	72.07	92.98
Transition strength, σt (MPa)	47.9	67.9	80.4

monomer prefers to be adsorbed on the montmorillonite and the interaction energy values obtained from the ab initio calculations are typical for the physical absorption for SWCNT-epoxy system where it was chemisorptions for montmorillonite-epoxy system. Also thermal and mechanical properties of SWCNT and MMT epoxy nanocomposites were tested in optimum loading of nanofillers. As it was predicted from calculations results, better improvement was achieved from MMT-epoxy nanocomposites rather than CNT-epoxy composites. This improvement would be caused of better interaction between montmorillonite surface and epoxy matrix. Finally, by performing thermal and mechanical analysis DFT calculation results have been proved.

Data Availability

The data used to support the findings of this study are available from the corresponding author upon request.

Conflicts of Interest

The authors declare that they have no conflicts of interest.

Acknowledgments

Support from University of Semnan and the Faculty of Engineering of University of Mazandaran is gratefully acknowledged.

References

[1] T. Wongjaiyen, W. Brostow, and W. Chonkaew, "Tensile properties and wear resistance of epoxy nanocomposites reinforced with cellulose nanofibers," *Polymer Bulletin*, vol. 75, no. 5, pp. 2039–2051, 2018.

[2] M. I. Kim, S. Kim, T. Kim, D. K. Lee, and B. Seo, "Mechanical and thermal properties of epoxy composites containing zirconium oxide impregnated halloysite nanotubes," *Coat*, vol. 7, no. 12, p. 231, 2017.

[3] M. S. Lakshmi, B. Narmadha, and B. S. R. Reddy, "Enhanced thermal stability and structural characteristics of different MMT-Clay/epoxy-nanocomposite materials," *Polymer Degradation and Stability*, vol. 93, pp. 201–213, 2008.

[4] H. Mahmood, S. H. Unterberger, and A. Pegoretti, "Tuning electrical and thermal properties in epoxy/glass composites by graphene-based interphase," *Journal of Composites Science*, vol. 1, no. 2, p. 12, 2017.

[5] X. Shi, T. A. Nguyen, Z. Suo, Y. Liu, and R. Avci, "Effect of nanoparticles on the anticorrosion and mechanical properties of epoxy coating," *Surface and Coatings Technology*, vol. 204, p. 237, 2009.

[6] D. Zaarei, F. Sharif, M. M. Gudarzi, and S. M. Kassiriha, "Using of p-phenylenediamine as modifier of montmorrilonite for preparation of epoxy-clay nanocomposites: morphology and solvent resistance properties," *Polymer-Plastics Technology and Engineering*, vol. 49, p. 285, 2010.

[7] B. Wetzel, P. Rosso, F. Haupert, and K. Friedrich, "Epoxy nanocomposites – fracture and toughening mechanisms," *Engineering Fracture Mechanics*, vol. 73, pp. 2375–2398, 2006.

[8] D. A. Hernandez, C. A. Soufen, and M. O. Orlandi, "Carbon fiber reinforced polymer and epoxy adhesive tensile test failure analysis using scanning electron microscopy," *Materials Research*, vol. 20, no. 4, pp. 951–961, 2017.

[9] Y. Huang, Y. Tian, Y. Li et al., "High mechanical properties of epoxy networks with dangling chains and tunable microphase separation structure," *RSC Advances*, vol. 7, no. 19, pp. 49074–49082, 2019.

[10] D. Shen, Z. Zhan, Z. Liu et al., "Enhanced thermal conductivity of epoxy composites filled with silicon carbide nanowires," *Scientific Reports*, vol. 7, p. 2606, 2017.

[11] G. R. Brubaker and D. W. Johnson, "Molecular mechanics calculations in coordination chemistry," *Coordination Chemistry Reviews*, vol. 53, pp. 1–36, 1984.

[12] M. Ionita and C. M. Damian, "Molecular modeling for calculation of mechanical properties of SWCNTs/epoxy composites: Effect of SWCNTs diameter," *Materiale Plastice*, vol. 48, no. 1, pp. 54–57, 2011.

[13] W. Peilin and L. Tran, "Molecule dynamics simulation of epoxy resin system," RECSEM-2017.

[14] X. Zhang, H. Wen, and Y. Wu, "Computational thermomechanical properties of silica–epoxy nanocomposites by molecular dynamic simulation," *Polymers*, vol. 9, no. 9, p. 430, 2017.

[15] N. Masghouni and M. A. Haik, "Computational molecular dynamics study of hybrid composite incorporating ZnO nanowires," *Journal of Computational and Theoretical Nanoscience*, vol. 12, p. 665, 2015.

[16] K. Fukuzawa, K. Kitaura, M. Uebayasi, K. Nakata, T. Kaminuma, and T. Nakano, "Ab initio quantum mechanical study of the binding energies of human estrogen receptor alpha with its ligands: an application of fragment molecular orbital method," *Journal of Computational Chemistry*, vol. 26, p. 1, 2005.

[17] K. Mylvaganam and L. C. Zhang, "Nanotube functionalization and polymer grafting: an ab initio study," *The Journal of Physical Chemistry B*, vol. 108, no. 39, pp. 15009–15012, 2004.

[18] D. W. Boukhvalov, D. R. Dreyer, C. W. Bielawski, and Y.-W. Son, "A computational investigation of the catalytic properties of graphene oxide: exploring mechanisms by using DFT methods," *ChemCatChem*, vol. 4, no. 11, pp. 1844–1849, 2012.

[19] A. Alemi, Z. Hosseinpour, M. Dolatyari, and A. Bakhtiari, "Boehmite (γ-AlOOH) nanoparticles: hydrothermal synthesis,

characterization, pH-controlled morphologies, optical properties, and DFT calculations," *Physica Status Solidi (b)*, vol. 249, no. 6, pp. 1264–1270, 2012.

[20] D. Singh, S. Ahmad, and P. P. Singh, "DFT based calculation of interaction energy between metal halides and organic bases," *Journal of Molecular Structure: THEOCHEM*, vol. 905, pp. 13–23, 2009.

[21] Ž. Šljivančanin, A. S. Milošević, Z. S. Popović, and F. R. Vukajlović, "Binding of atomic oxygen on graphene from small epoxy clusters to a fully oxidized surface," *Carbon*, vol. 54, pp. 482–488, 2013.

[22] M. G. Ahangari, A. Fereidoon, M. Jahanshahi, and M. D. Ganji, "Electronic and mechanical properties of single-walled carbon nanotubes interacting with epoxy: A DFT study," *Physica E: Low-Dimensional Systems and Nanostructures*, vol. 48, pp. 148–156, 2013.

[23] M. Elstner, D. Porezag, G. Jungnickel et al., "Self-consistent-charge density-functional tight-binding method for simulations of complex materials properties," *Physical Review B: Condensed Matter and Materials Physics*, vol. 58, no. 11, pp. 7260–7268, 1998.

[24] B. Aradi, B. Hourahine, and T. Frauenheim, "DFTB+, a sparse matrix-based implementation of the DFTB method," *The Journal of Physical Chemistry A*, vol. 111, no. 26, 2007.

[25] P. Hohenberg and W. Kohn, "Inhomogeneous electron gas," *Physical Review B*, vol. 136, pp. B864–B871, 1964.

[26] W. Kohn, "Nobel lecture: electronic structure of matter—wave functions and density functionals," *Reviews of Modern Physics*, vol. 71, p. 1253, 1999.

[27] P. Ordejón, E. Artacho, and J. M. Soler, "Self-consistent order-*N* density-functional calculations for very large systems," *Physical Review B: Condensed Matter and Materials Physics*, vol. 53, no. 16, pp. R10441–R10444, 1996.

[28] J. M. Soler, E. Artacho, J. D. Gale et al., "The SIESTA method for ab initio order-N materials simulation," *Journal of Physics: Condensed Matter*, vol. 14, no. 11, pp. 2745–2779, 2002.

[29] J. P. Perdew, K. Burke, and M. Ernzerhof, "Generalized gradient approximation made simple," *Physical Review Letters*, vol. 77, no. 18, pp. 3865–3868, 1996.

[30] A. Viani, A. Gualtieri, and G. Artioli, "The nature of disorder in montmorillonite by simulation of X-ray powder patterns," *American Mineralogist*, vol. 87, no. 7, pp. 966–975, 2002.

[31] F. Jensen, "An atomic counterpoise method for estimating inter- and intramolecular basis set superposition errors," *Journal of Chemical Theory and Computation*, vol. 6, no. 1, pp. 100–106, 2010.

[32] G. Kresse, A. Gil, and P. Sautet, "Significance of single-electron energies for the description of CO on Pt(111)," *Physical Review B: Condensed Matter and Materials Physics*, vol. 68, no. 7, pp. 73401–73405, 2003.

[33] M. Rudolph and E. L. Ratcliff, "Normal and inverted regimes of charge transfer controlled by density of states at polymer electrodes," *Nature Communications*, vol. 8, pp. 1048–1052, 2017.

[34] L. S. Schadler, L. C. Brinson, and W. G. J. Sawyer, "Polymer nanocomposites: a small part of the story," *Journal of the Minerals Metals & Materials Society*, vol. 59, no. 3, pp. 53–60, 2007.

[35] W. R. Caseri, "Nanocomposites of polymers and inorganic particles: preparation, structure and properties," *Materials Science and Technology*, vol. 22, no. 7, pp. 807–817, 2006.

[36] L. S. Schadler, S. K. Kumar, B. C. Benicewicz, S. L. Lewis, and S. E. Harton, "Designed interfaces in polymer nanocomposites: a fundamental viewpoint," *Materials Research Bulletin*, vol. 32, pp. 335–340, 2007.

[37] B. Pukanski and E. Fekete, "Adhesion and surface modification," *Advances in Polymer Science*, vol. 139, pp. 109–153, 1999.

[38] X. Kornmann, H. Lindberg, and L. A. Berglund, "Synthesis of epoxy-clay nanocomposites: influence of the nature of the clay on structure," *Polymer Journal*, vol. 42, no. 4, pp. 1303–1310, 2001.

[39] A. Yasmin, J. L. Abot, and I. M. Daniel, "Processing of clay/epoxy nano-composites with a three-roll mill machine," *Materials Research Society Symposium Proceedings*, vol. 740, pp. 75–80, 2003.